Official Journal of CIOMP
elight.springeropen.com

RESEARCH ARTICLE

Open Access

Scalar optical hopfions

Chenhao Wan[1,2*], Yijie Shen[3], Andy Chong[4] and Qiwen Zhan[1,5,6*]

Abstract

Hopfions are three-dimensional (3D) topological states discovered in field theory, magnetics, and hydrodynamics that resemble particle-like objects in physical space. Hopfions inherit the topological features of the Hopf fibration, a homotopic mapping from unit sphere in 4D space to unit sphere in 3D space. Here we design and demonstrate dynamic scalar optical hopfions in the shape of a toroidal vortex and expressed as an approximate solution to Maxwell's equations. Equiphase lines correspond to disjoint and interlinked loops forming complete ring tori in 3D space. The Hopf invariant, product of two winding numbers, is determined by the topological charge of the poloidal spatiotemporal vortices and toroidal spatial vortices in toroidal coordinates. Optical hopfions provide a photonic testbed for studying topological states and may be utilized as high-dimensional information carriers.

Keywords: Hopfion, Toroidal vortex, Spatiotemporal vortex, Wave packet, Topology, Topological charge

1 Introduction

The knot theory originates in Lord Kevin's model proposed in 1867 that atoms are made of vortex rings or vortex knots [1]. Although the hypothesis was proved to be unsuccessful, the knot theory has since then proliferated in both mathematics and physics [2,3]. One peculiar category of knots—the torus knots—are disjoint and linked closed loops, nesting to construct complete ring tori. Physicists find the torus knot a suitable candidate for building hopfions—three-dimensional (3D) topological states that resemble particle-like objects.

Hopfions are named after Heinz Hopf who discovered the Hopf fibration in 1931 [4]. The Hopf fibration delineates an elegant mapping from unit sphere in 4D space (S^3) to unit sphere in 3D space (S^2), belonging to the third homotopy group $\pi_3(S_2) = \mathbb{Z}$ [5–7]. The preimages of any arbitrary points in S^2 are disjoint and interlinked circles (S^1) in S^3. The S^3 that resides in four-dimensional space can be "seen" by the use of stereographic projection and the topological features of linkedness of closed loops are preserved.

*Correspondence: wanchenhao@hotmail.com; qwzhan@usst.edu.cn

[1] School of Optical-Electrical and Computer Engineering, University of Shanghai for Science and Technology, Shanghai 200093, China
Full list of author information is available at the end of the article

The search of hopfions in physical systems started with the seminal work of Korepin and Faddeev [8] and after nearly half a century, hopfions have been unveiled in various branches of science. Hopf structures are discovered in superfluid helium as particle-like objects with finite dimension and energy [9]. Null solutions to Maxwell's equations reveal that electromagnetic field lines, spin or polarization vectors can be tied based on the Hopf fibration to form diverse knots and links and exploited as information carriers [10–19]. Vortex lines in fluids appear in Hopf topological structures and the linkedness as well as knottedness are conserved in inviscid fluids [20]. Topological defect lines in liquid crystals are tweezed to create Hopf links [21–23]. The abovementioned hopfions are vector hopfions that each point in S^2 corresponds to a vector that has multiple degrees of freedom. On the contrary, each point in S^2 of scalar hopfions is distinguished by the value of a scalar parameter. The corresponding preimage is a closed loop consisting of all points having the same scalar value. Scalar hopfions have been predicted and are believed to be experimentally feasible in a Bose-Einstein condensate (BEC) controlled by inhomogeneous magnetic fields or in a rotating trapped atomic BEC [24,25].

Particle-like topological objects such as skyrmions have attracted considerable interest in light science in recent

years [26–30] because of their nano size and topological stability. A skyrmion can be described by knots of twisting field lines. Hopfions are topological objects that can be formed from a closed loop of twisted skyrmion strings [17]. Last year, Sugic et al. synthesized the transverse states of polarization and the phase profile into a Hopf fibration texture in the focal volume [31], which was recently extended to higher-order cases [32].

Rather than steady-state continue-wave structured light, the concept of scalar optical hopfions proposed in the current paper is spatiotemporally structured pulse propagating in space-time, providing an additional dimension (time) to encode and transfer topological information. The dynamic scalar optical hopfion is a travelling wave packet in the shape of a toroidal vortex. Scalar optical hopfions are weaved by nested equiphase lines that each equiphase line corresponds to one complex knot or several unknotted and interlinked closed loops. The linking number of two equiphase lines is governed by the Hopf invariant that is the product of the winding numbers. All equiphase lines form an infinite number of layers of complete ring tori. The discovery of scalar optical hopfions may spur interest in exploring novel methods for light-matter interaction, optical metrology, information encoding, and optical manipulation [33–38].

2 Results and discussion

The envelope function of a light field in a uniform medium with anomalous group velocity dispersion (GVD) in Cartesian coordinates is expressed as [39,40],

$$i\frac{\partial\psi}{\partial z}+\frac{1}{2k}\left(\frac{\partial^2\psi}{\partial x^2}+\frac{\partial^2\psi}{\partial y^2}\right)-\frac{k_2}{2}\frac{\partial^2\psi}{\partial\tau^2}=0, \tag{1}$$

where ψ is the wave function, x, y, and z are Cartesian coordinates, τ is the retarded time in the local frame, k is the wave number, k_2 is the GVD at $\omega=\omega_0$. Equation (1) can be normalized with regard to the dimensions of the wave packet and reads,

$$\frac{\partial^2\psi}{\partial X^2}+\frac{\partial^2\psi}{\partial Y^2}+\frac{\partial^2\psi}{\partial \mathrm{T}^2}+2i\frac{\partial\psi}{\partial Z}=0, \tag{2}$$

where $X=\frac{x}{x_s}$, $Y=\frac{y}{x_s}$, $\mathrm{T}=\frac{\tau}{\tau_s}$, and $Z=\frac{z}{z_R}$. Here x_s and τ_s are the dimensions of the wave packet along the x and τ directions, z_R denotes the Rayleigh range. The dimensions in x and y directions are assumed to be equal. k_2 is negative so that the spatial and temporal second derivatives share the same sign, $|k_2|=\frac{\tau_s^2}{kx_s^2}$. An approximate solution to Eq. (2) can be expressed as:

$$\psi_{z=0}=\left(\frac{\sqrt{(r_\perp-r_0)^2+\mathrm{T}^2}}{\sqrt{z_0}}\right)^{|l_2|}\exp\left(-\frac{(r_\perp-r_0)^2+\mathrm{T}^2}{2z_0}\right)\exp\left(-il_2\tan^{-1}\left(\frac{\mathrm{T}}{r_\perp-r_0}\right)\right)\exp\left(il_1\tan^{-1}\left(\frac{y}{x}\right)\right), \tag{3}$$

where $r_\perp=\sqrt{x^2+y^2}$, r_0 and z_0 are constants, l_1 and l_2 are integers. Equation (3) is the wave function of a scalar optical hopfion in the shape of a toroidal vortex. As shown in Fig. 1, a scalar hopfion consists of an infinite number of layers of tori. Each torus are weaved by closed loops. Each closed loop is painted in one specific color and corresponds to a point in the parameter space and to a circle on unit sphere in 4D space. Each closed loop of a scalar hopfion is an equiphase line. As presented in Eq. (3), the phase of a scalar hopfion is the sum of a spatial spiral phase with topological charge l_1 and a spatiotemporal spiral phase with topological charge l_2. The two numbers are also known as the winding numbers defined as,

$$l_1=\frac{1}{2\pi}\oint_C\nabla\phi_{x,y}(\boldsymbol{r}_{tor})d\boldsymbol{r}_{tor}, \tag{4}$$

$$l_2=\frac{1}{2\pi}\oint_C\nabla\phi_{r_\perp-r_0,\mathrm{T}}(\boldsymbol{r}_{pol})d\boldsymbol{r}_{pol}, \tag{5}$$

where ∇ is the nabla operator, $\boldsymbol{r}_{tor}$ and $\boldsymbol{r}_{pol}$ are the position vectors in the toroidal plane and poloidal plane,

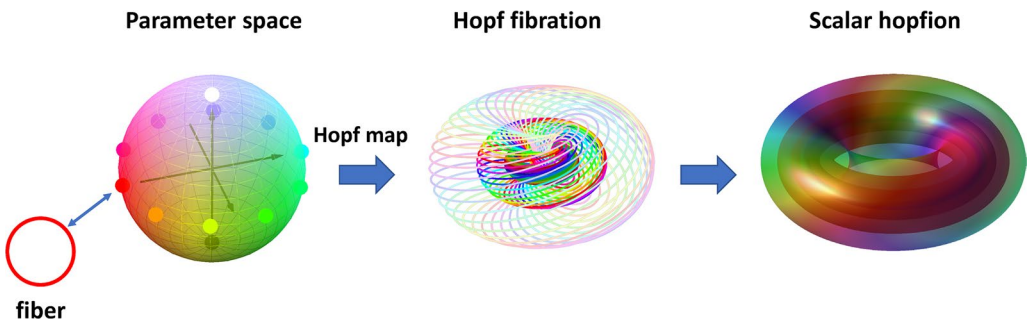

Fig. 1 Schematic of the Hopf fibration and scalar hopfion. The equiphase lines in a scalar hopfion presents the topological features of the Hopf fibration

respectively. The Hopf invariant is defined as the product of the two winding numbers:

$$Q_{Hopf} = l_1 l_2 \tag{6}$$

.

For any ring torus in 3D space, equiphase points of a scalar optical hopfion form closed loops. Note that a ring torus is a surface not a solid. As shown in Fig. 2a, the red loop consists of all points in the green ring torus that have the phase value of 1.5; the blue loop represents equiphase points for phase value of 3. The two loops are disjoint and linked only once. The linking number is governed by the Hopf index that is $l_1 \times l_2 = 1$ for this case. In Fig. 2b, both winding numbers are 2. Instead of being one closed loop, the red equiphase lines are actually two closed loops linked to each other once. Consequently, the red and blue equiphase lines are linked four times. The linking number is consistent with the Hopf index $l_1 \times l_2 = 4$. In Fig. 2c, the winding number l_1 is 2 and l_2 is 3. The equiphase line is a knot winding about the ring twice and about the hole triple times. The red and blue knots are linked to each other 6 times. In Fig. 2d, the winding number l_1 is 4 and l_2 is 2. The equiphase lines are composed of two disjoint and linked closed loops. Taking the red curves for example, each of the pair of red loops winds about the ring twice and about the hole once. The red loops and the blue loops are linked $2 \times 2 \times 2 = 8$ times that is consistent with the Hopf index $l_1 \times l_2 = 8$. It is obvious from the above examples that the linking number of equiphase loops are equal to the Hopf invariant that is the product of the two winding numbers. The equiphase line may be one closed loop or split into several disjoint and linked closed loops. The number of disjoint loops of one specific equiphase line is equal to the greatest common divider of the two winding numbers. For example, the greatest common divider in Fig. 2d is 2, therefore, the red curves are composed of two disjoint and linked loops. If both winding numbers are greater than 1 and their greatest common divider is 1, the equiphase line turns out to be an optical knot. Additional examples can be found in the supplementary information (Additional file 1).

Disjoint and linked loops are one distinct feature of hopfions. Another peculiar feature is that these disjoint and linked loops form complete ring tori. In Fig. 3, four examples of hopfions with different sets of winding numbers are presented. A total of 50 equiphase lines are plotted for each graph. The phase values are equally spaced and listed on the right side of the figures. Evidently, regardless of the combination of the two winding numbers, all equiphase lines form a complete ring torus. A

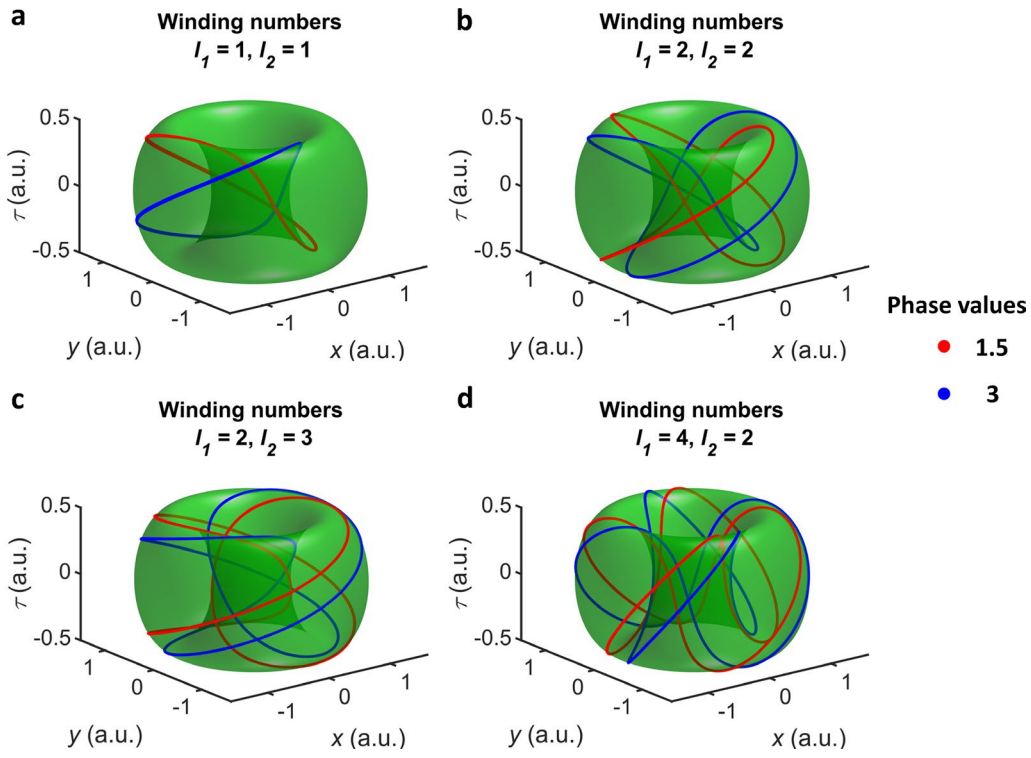

Fig. 2 Optical hopfions showing two equiphase lines with winding numbers: **a** $l_1 = 1, l_2 = 1$. **b** $l_1 = 2, l_2 = 2$. **c** $l_1 = 2, l_2 = 3$. **d** $l_1 = 4, l_2 = 2$

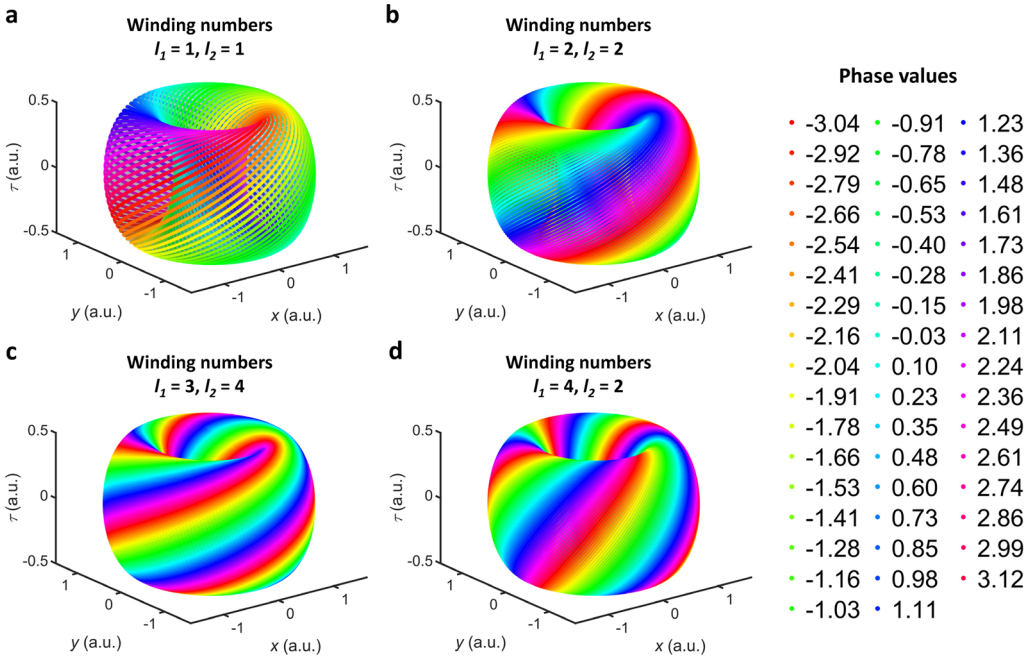

Fig. 3 Optical hopfions showing 50 equiphase lines to form ring tori with winding numbers: **a** $l_1 = 1, l_2 = 1$. **b** $l_1 = 2, l_2 = 2$. **c** $l_1 = 3, l_2 = 4$. **d** $l_1 = 4, l_2 = 2$

ring torus is a surface created by rotating a circle about an axis in the same plane as the circle in 3D space. The radius of the circle is always smaller than the distance between the center of the circle and the rotating axis, i.e., the poloidal radius is always smaller than the toroidal radius for a ring torus. It is of great importance to note that regardless of the shape and size of the ring torus, the two distinct features of hopfions are always valid. In other words, equiphase lines form complete and infinite number of layers of tori in 3D space with disjoint and interlinked closed loops. The Hopf index judges the linking number of any pair of individual loops corresponding to different scalar values.

The key to experimentally generate optical hopfions is to manipulate poloidal and toroidal spiral phase in toroidal coordinates. A linear method has recently been demonstrated to create toroidal vortices of light [41]. As shown in Fig. 4, through manipulating spiral phase in the *k*-space by the use of a two-dimensional pulse shaper consisting of a grating, a cylindrical lens and a spatial light modulator (SLM1), a fully controlled twisted phase is generated in the spatiotemporal domain. The spatiotemporal optical vortex (STOV) is experimentally elongated to a STOV tube along the vortex line by two cylindrical lenses in a confocal configuration. The STOV tube is wrapped into a toroidal vortex through conformal mapping by SLM2 and SLM3. SLM2 performs the log-polar to Cartesian coordinate transformation. SLM3 corrects the phase and applies a toroidal spiral phase. SLM3 and SLM1 control the two winding numbers l_1 and l_2, respectively. Both winding numbers can be arbitrary integer with both signs. However, high-order STOVs tend to split upon free-space propagation. Choosing proper negative GVD materials or preconditioning the controlled phase imprinted by SLM1 can circumvent the problem [42,43].

Characterization of a scalar optical hopfion is a challenging task that requires high-resolution and full 3D phase measurement of an ultrafast wave packet. Limited by existing capabilities, we perform two-dimensional phase measurement of the poloidal spiral phase through interfering the hopfion wave packet ($l_1 = 1$, $l_2 = 1$) with a transform-limited reference pulse split from the source. The reference pulse is considerably shorter in time and interferes with each temporal slice of the hopfion wave packet with the help of an electronically controlled precision stage. The poloidal phase is theoretically a spiral phase in the spatiotemporal domain. Eight spots at equally-spaced toroidal angles are chosen and the interference patterns at these spots are analyzed. Figure 5a shows an example of the interference patterns obtained at the toroidal angle of 112.5 degrees. The orientations of mirrors are carefully adjusted so that the fringes are parallel to the specified

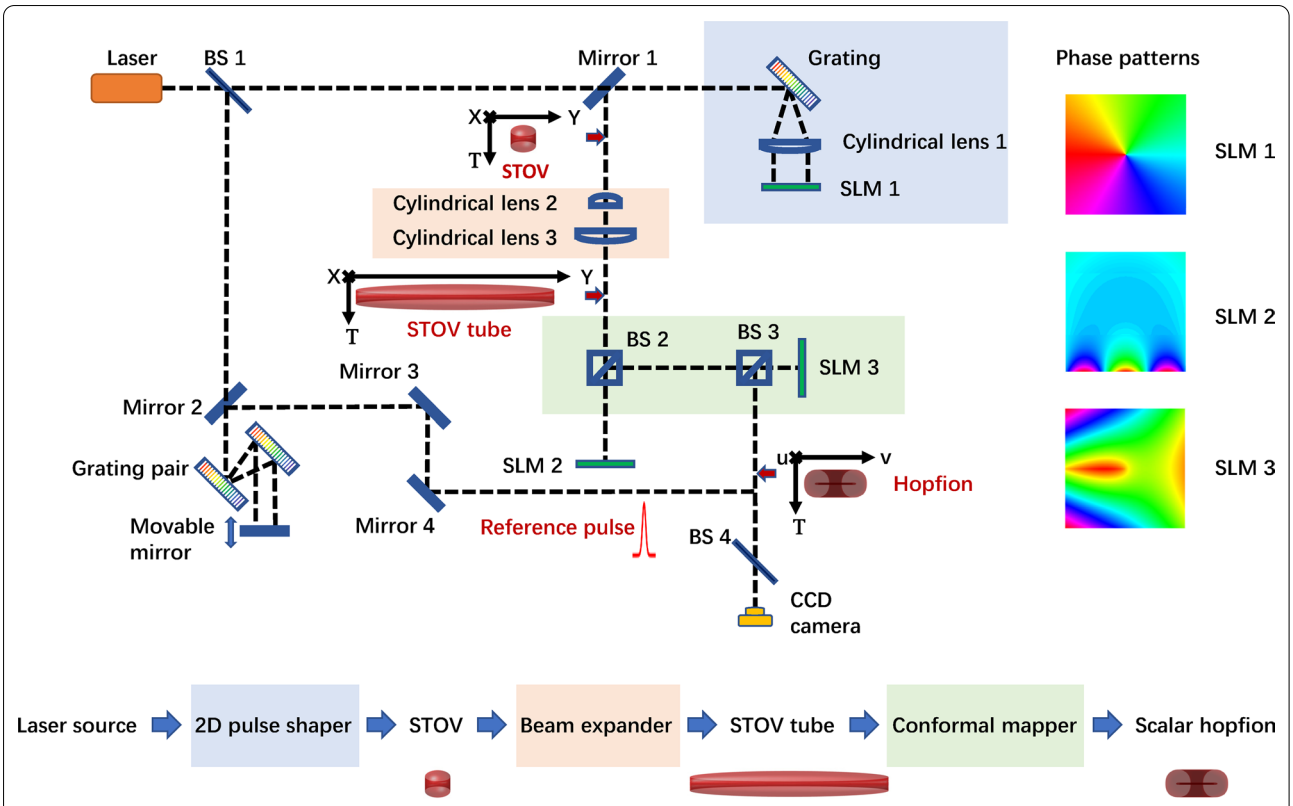

Fig. 4 Schematic of the experimental setup for the generation and characterization of optical hopfions. A chirped pulse is transformed to a STOV by the use of a two-dimensional pulse shaper, elongated to a STOV tube and conformally mapped to an optical hopfion. BS: beam splitter; SLM: spatial light modulator

toroidal angle. As the reference pulse interferes with the head of the hopfion wave packet, the fringe patterns are straight lines (label 1). Approaching the center of the spatiotemporal vortex, the fringes start to bend (label 2). When the temporal slice is coincident with the vortex core, the upper and lower fringes are shifted by half a period (label 3). The shifting is caused by the π difference between the upper and lower fringes, a salient feature of a spatiotemporal vortex of topological charge 1. As the temporal slicing continues, the fringes bend to the opposite direction (label 4) and become straight again as the slicing approaches the tail of the hopfion wave packet (label 5). Based on the fringe patterns, the poloidal spiral phase can be reconstructed. The toroidal spiral phase is a spatial spiral phase applied by SLM3 and assumed to be perfect in this case due to the difficulties of fully resolving the 3D details of the phase distributions of the entire wave packet. The total phase is the sum of the poloidal phase and the toroidal phase. Figure 5b shows the theoretical equiphase curves plotted in solid lines and the experimental phase data denoted by circles. The topological features of a scalar optical hopfion are clearly presented.

3 Conclusion

In summary, we propose a dynamic scalar optical hopfion model and provides its analytical expression as an approximate solution to Maxwell's equations. Numerical simulations and experimental data demonstrate that the equiphase lines are disjoint and linked closed loops in the form of links and knots with a linking number determined by the Hopf invariant. All equiphase loops form complete tori that fill up the entire 3D space. The dynamic scalar optical hopfions provide a photonic testbed for studying topological states that resemble particle-like objects, and may find applications in spatiotemporal mode excitation in artificial materials and nanostructures, and in optical communication as high-dimensional information carriers.

4 Methods

The fiber laser is dispersion-managed and mode-locked with a central wavelength of 1030 nm. The model of the SLMs is GAEA-2-NIR-069 made by Holoeye. A

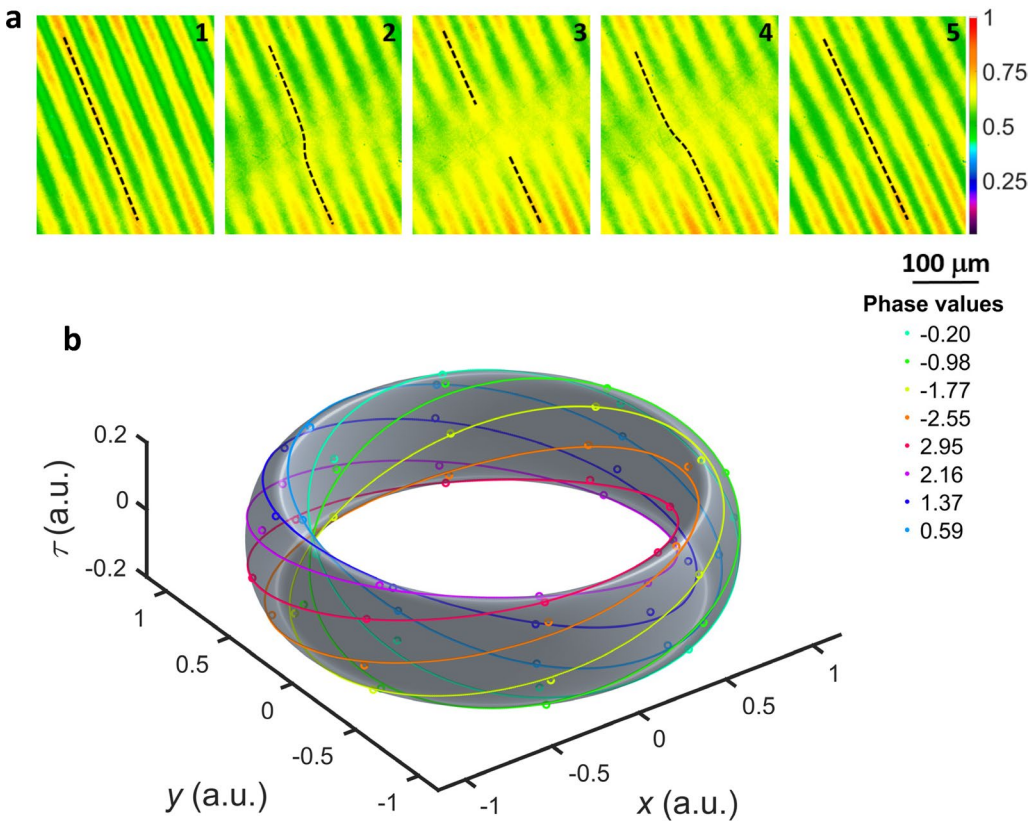

Fig. 5 Experimental results of a scalar optical hopfion ($l_1 = 1$, $l_2 = 1$). **a** Interference fringe patterns for phase measurements. **b** Theoretical equiphase curves of a hopfion are plotted in solid curves. Experimental data are denoted by circles. Each color corresponds to one specific phase value

Gaussian pulse is converted to a STOV pulse through a 2D pulse shaper. The STOV pulse is elongated to a STOV tube through two cylindrical lenses. The STOV tube is conformally mapped to a scalar hopfion using SLM2 and SLM3. The characterization is performed by interference with a transform-limited reference pulse split from the source. The temporal scan is controlled by an electrical precision stage (Zolix MAR20-65). The phase reconstruction is based on all the fringe patterns measured at 8 equally spaced toroidal angles during the temporal scan.

Abbreviations

3D: Three dimension; BEC: Bose-Einstein condensate; GVD: Group velocity dispersion; STOV: Spatiotemporal optical vortex; SLM: Spatial light modulator.

Supplementary Information

The online version contains supplementary material available at https://doi.org/10.1186/s43593-022-00030-2.

Additional file 1. Fig. S1. Schematic of three related optical wave packets. Fig. S2. Optical hopfions showing two equiphase lines with winding numbers: a, l1 = 1, l2 = 1. b, l1 = 2, l2 = 1. c, l1 = 3, l2 = 1. d, l1 = 4, l2 = 1. Fig. S3. Optical hopfions showing two equiphase lines with winding numbers: a, l1 = 1, l2 = 2. b, l1 = 1, l2 = 3. c, l1 = 1, l2 = 4. d, l1 = 2, l2 = 2. Fig. S4. Optical hopfions showing two equiphase lines with winding numbers: a, l1 = 3, l2 = 3. b, l1 = 2, l2 = 3. c, l1 = 4, l2 = 2. d, l1 = 4, l2 = 3. Fig. S5. Optical hopfions showing 50 equiphase lines to form ring tori with winding numbers: a, l1 = 1, l2 = 1. b, l1 = 3, l2 = 1. c, l1 = 1, l2 = 2. d, l1 = 1, l2 = 4. Fig. S6. Optical hopfions showing 50 equiphase lines to form ring tori with winding numbers: a, l1 = 2, l2 = 2. b, l1 = 4, l2 = 2. c, l1 = 3, l2 = 3. d, l1 = 3, l2 = 4.

Acknowledgements

Not applicable.

Author contributions

CW, YS, AC and QZ initiated the original idea. CW and YS performed the theoretical analysis and numerical simulations. CW performed the experiments. CW and QZ analyzed the experimental results. QZ guided the theoretical analysis and supervised the project. All authors contributed to writing the manuscript. All authors read and approved the final manuscript.

Funding

We acknowledge the support from the National Natural Science Foundation of China (NSFC) (92050202 (Q.Z.), 61875245 (C.W.)), Shanghai Science and Technology Committee (19060502500 (Q.Z.)), and Wuhan Science and Technology Bureau (2020010601012169 (C.W.)).

Data availability

All data presented in the report are available upon reasonable request.

Declarations

Ethics approval and consent to participate
Not applicable.

Consent for publication
Not applicable.

Competing interests
Authors declare no competing interests.

Author details
[1]School of Optical-Electrical and Computer Engineering, University of Shanghai for Science and Technology, Shanghai 200093, China. [2]School of Optical and Electronic Information and Wuhan National Laboratory for Optoelectronics, Huazhong University of Science and Technology, Wuhan 430074, Hubei, China. [3]Optoelectronics Research Centre, University of Southampton, Southampton SO17 1BJ, UK. [4]Department of Physics, Pusan National University, Geumjeong-Gu, Busan 46241, South Korea. [5]Zhangjiang Laboratory, 100 Haike Road, Shanghai 201204, China. [6]Shanghai Key Lab of Modern Optical System, University of Shanghai for Science and Technology, Shanghai 200093, China.

Received: 11 August 2022 Revised: 10 September 2022 Accepted: 14 September 2022
Published online: 01 November 2022

References

1. W. Thomson, On vortex atoms. Phil. Mag. **34**, 15–24 (1867)
2. N. Manton, P. Sutcliffe, *Topological Solitons* (Cambridge Univ Press, Cambridge, 2004)
3. L.H. Kauffman, *Knots and Physics* (World Scientific Publishing, Singapore, 2001)
4. H. Hopf, Über die Abbildungen der dreidimensionalen Sph'dre aufdie Kugelfidche. Math. Ann. **104**, 637–665 (1931)
5. J.S.B. Tai, I.I. Smalyukh, Static Hopf solitons and knotted emergent fields in solid-state noncentrosymmetric magnetic nanostructures. Phys. Rev. Lett. **121**, 187201 (2018)
6. P.J. Ackerman, I.I. Smalyukh, Diversity of knot solitons in liquid crystals manifested by linking of preimages in torons and hopfions. Phys. Rev. X **7**, 011006 (2017)
7. S. Castillo-Sepúlveda, R. Cacilhas, V.L. Carvalho-Santos, R.M. Corona, D. Altbir, Magnetic hopfions in toroidal nanostructures driven by an Oersted magnetic field. Phys. Rev. B **104**, 184406 (2021)
8. V.E.E. Korepin, L.D. Faddeev, Quantization of solitons. Theor. Math. Phys. **25**, 1039–1049 (1975)
9. G.E. Volovik, V.P. Mineev, Particle-like solitons in superfluid ^{3}He phases. Zh Eksp. Teor Fiz. **73**, 767–773 (1977)
10. L. Faddeev, A.J. Niemi, Stable knot-like structures in classical field theory. Nature **387**, 58–61 (1997)
11. A.F. Ranada, A topological theory of the electromagnetic field. Lett. Math. Phys. **18**, 97–106 (1989)
12. W.T. Irvine, Linked and knotted beams of light, conservation of helicity and the flow of null electromagnetic fields. J. Phys. A Math. Theor. **43**, 385203 (2010)
13. W. Irvine, D. Bouwmeester, Linked and knotted beams of light. Nat. Phys. **4**, 716–720 (2008)
14. H. Kedia, I. Bialynicki-Birula, D. Peralta-Salas, W.T. Irvine, Tying knots in light fields. Phys. Rev. Lett. **111**, 150404 (2013)
15. P.J. Ackerman, I.I. Smalyukh, Static three-dimensional topological solitons in fluid chiral ferromagnets and colloids. Nat. Mater. **16**, 426–432 (2017)
16. X.S. Wang, A. Qaiumzadeh, A. Brataas, Current-driven dynamics of magnetic hopfions. Phys. Rev. Lett. **123**, 147203 (2019)
17. N. Kent et al., Creation and observation of Hopfions in magnetic multilayer systems. Nat. Commun. **12**, 1–7 (2021)
18. Y. Liu, W. Hou, X. Han, J. Zang, Three-dimensional dynamics of a magnetic hopfion driven by spin transfer torque. Phys. Rev. Lett. **124**, 127204 (2020)
19. I. Luk'Yanchuk, Y. Tikhonov, A. Razumnaya, V.M. Vinokur, Hopfions emerge in ferroelectrics. Nat. Commun. **11**, 1–7 (2020)
20. D. Kleckner, W. Irvine, Creation and dynamics of knotted vortices. Nat. Phys. **9**, 253–258 (2013)
21. I.I. Smalyukh, Y. Lansac, N.A. Clark, R.P. Trivedi, Three-dimensional structure and multistable optical switching of triple-twisted particle-like excitations in anisotropic fluids. Nat. Mater. **9**, 139–145 (2010)
22. U. Tkalec, M. Ravnik, S. Čopar, S. Žumer, I. Muševič, Reconfigurable knots and links in chiral nematic colloids. Science **333**, 62–65 (2011)
23. H.R. Sohn et al., Dynamics of topological solitons, knotted streamlines, and transport of cargo in liquid crystals. Phys. Rev. E **97**, 052701 (2018)
24. Y.V. Kartashov, B.A. Malomed, Y. Shnir, L. Torner, Twisted toroidal vortex solitons in inhomogeneous media with repulsive nonlinearity. Phys. Rev. Lett. **113**, 264101 (2014)
25. Y.M. Bidasyuk et al., Stable Hopf solitons in rotating Bose-Einstein condensates. Phys. Rev. A **92**, 053603 (2015)
26. S. Tsesses, E. Ostrovsky, K. Cohen, B. Gjonaj, N.H. Lindner, G. Bartal, Optical skyrmion lattice in evanescent electromagnetic fields. Science **361**(6406), 993–996 (2018)
27. L. Du, A. Yang, A.V. Zayats, X. Yuan, Deep-subwavelength features of photonic skyrmions in a confined electromagnetic field with orbital angular momentum. Nat. Phys. **15**, 650–654 (2019)
28. Z.L. Deng, T. Shi, A. Krasnok, X. Li, A. Alù, Observation of localized magnetic plasmon skyrmions. Nat. Commun. **13**, 1–7 (2022)
29. Y. Shen, Y. Hou, N. Papasimakis, N. Zheludev, Supertoroidal light pulses as electromagnetic skyrmions propagating in free space. Nat. Commun. **12**, 1–9 (2021)
30. Y. Shen, E.C. Martínez, C. Rosales-Guzmán, Generation of optical skyrmions with tunable topological textures. ACS Photon. **9**, 296–303 (2022)
31. D. Sugic et al., Particle-like topologies in light. Nat. Commun. **12**, 1–10 (2021)
32. Y. Shen et al., Topological transformation and free-space transport of photonic hopfions. https://arxiv.org/abs/2207.05074
33. M.R. Dennis, R.P. King, B. Jack, K. O'holleran, M.J. Padgett, Isolated optical vortex knots. Nat. Phys. **6**, 118–121 (2010)
34. L.J. Kong et al., High capacity topological coding based on nested vortex knots and links. Nat. Commun. **13**, 1–8 (2022)
35. H. Larocque et al., Reconstructing the topology of optical polarization knots. Nat. Phys. **14**, 1079–1082 (2018)
36. H. Larocque et al., Optical framed knots as information carriers. Nat. Commun. **11**, 1–8 (2020)
37. J.A. Rodrigo, T. Alieva, Freestyle 3D laser traps: tools for studying light-driven particle dynamics and beyond. Optica **2**, 812–815 (2015)
38. J.A. Rodrigo, T. Alieva, E. Abramochkin, I. Castro (2013). Shaping of light beams along curves in three dimensions. *Opt. Express* **21**, 20544–20555 (2013)
39. M.S. Mills et al., Localized waves with spherical harmonic symmetries. Phys. Rev. A **86**, 063811 (2012)
40. O.V. Borovkova, Y.V. Kartashov, V.E. Lobanov, V.A. Vysloukh, L. Torner, General quasi-nonspreading linear three-dimensional wave packets. Opt. Lett. **36**, 2176–2178 (2011)
41. C. Wan, Q. Cao, J. Chen, A. Chong, Q. Zhan, Toroidal vortices of light. Nat. Photonics **16**, 519–522 (2022)
42. Q. Cao et al., Non-spreading Bessel spatiotemporal optical vortices. Sci. Bull. **67**, 133–140 (2022)
43. W. Chen et al., Time diffraction-free transverse orbital angular momentum beams. Nat. Commun. **13**, 1–9 (2022)

Publisher's Note